Particle Dampers for Pump Noise Mitigation: Experimental Investigation of the Effects on Airborne and Structure-Borne Noise and Sound Perception on an Axial Piston Pump

Michael Lenz , Peter Zuppke , and Jürgen Weber

Chair of Fluid-Mechatronic Systems, TU Dresden, Germany
E-mail: michael.g.e.lenz@tu-dresden.de; juergen.weber@tu-dresden.de

Abstract

The reduction of noise emissions is a central target in positive displacement pump design, and the mitigation of structure borne noise is a main approach toward that goal. Particle damping offers a passive means of vibration mitigation without input energy requirement nor compromising the pump function and efficiency. The principle was applied to an axial piston pump and tested in sound power and structure borne noise measurements. A hollow encasing, which envelops most of the pump's sound emitting surface, is mounted, simultaneously providing particle damping and vibration decoupling properties. Finally, damping cavities are introduced modifying the pump's swash plate and end casing. Design considerations and experimental performance of the particle dampers with regards to sound power, sound quality, structure borne noise, and modal behaviour are presented and discussed. The mounted particle damped encasing provides a marked reduction of emitted sound power and improved sound quality. Meanwhile, no systematic acoustic improvement was observed for the particle dampers in the swash plate and end casing, which may be attributable to the pump's modal behaviour.

Keywords: NVH, pump noise mitigation, particle damping, sound perception / psychoacoustics

1 Introduction

The emitted noise of machines in operation is a central criterion for user satisfaction and acceptance. Exposure to high sound pressure level noise will lead to discomfort and possibly adverse health effects. Annoyance from noise is not solely a function of the integral sound pressure level, but may also be determined by the spectral distribution of sound pressure as well as swelling and transient effects. Also, personal sensitivity of auditors to sound characteristics will vary. The study of sound quality perception, as the correlation between objectively determinable characteristics of sound pressure signals and individual human sensation, is part of the field of psychoacoustics (e.g. [1, 2]).

Positive displacement pumps are frequently the dominant noise source of hydraulic drive systems. This is especially true for modern electrified drives, due to the disappearance of the prominent noise contribution of combustion engines and its masking effect. Pumps contribute to noise emissions by radiating airborne sound, as well as by inducing fluid and structure borne noise into adjacent components. Noise and vibration mitigation is therefore a central design goal for displacement pumps.

An effective approach is to tackle vibrations at their source, i.e. to optimize the drive geometry for minimal vibration excitation due to pressure build-up and flow pulsations, e.g. [3–7] . However, a base level of vibration excitation remains unavoidable due to the working principles of displacement pumps, and these mitigation measures are limited by the potential of additional leakage and resulting reduced pump efficiency. As an example, relief grooves in axial piston pump valve plates provide for a smoothed pressure build-up, but over a threshold length cause cross-porting and resulting internal leakage [3, 5, 8].

Active suppression of fluid [9] and structure borne [10] oscillations can yield significant attenuation effects, but may require costly additional electronic and machine components, which also potentially increase the sound emitting surface significantly as well as overall system complexity. In contrast, passive mitigation strategies do not require steering energy and can typically be realized with comparatively simple components. A classical example is resonance avoidance by tuning the natural frequencies of the pump and the attached hydraulic system so that they don't overlap with pump displacement frequencies and their higher orders; however this approach is much more complicated for variable speed modes of opera-

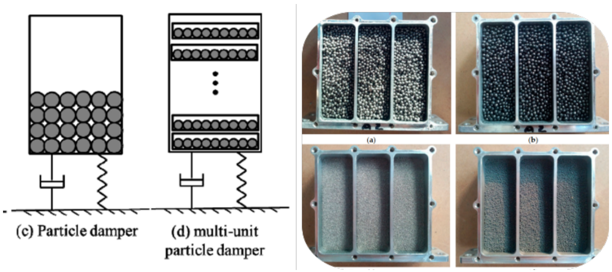

Figure 1: Working principle of particle damping, from [12]

tion which are gaining relevance in the context of electrification, as the spectrum of excitation frequencies becomes broadband. Other passive measures typically operate on the periphery of the pump and include the use of elastic hoses and motor pump unit bushings for vibration isolation or decoupling, silencers and Helmholtz resonators, acoustic insulation and barriers [11].

Particle dampers represent a further emerging means of structure borne noise mitigation. Figure 1 shows the basic setup: hollow spaces in the vibrating structure are partially filled with loose particles. Kinetic vibration energy is transmitted from the walls into the particles, resulting in chaotic or semi-structured [13] relative movement of the particle bed. Due to friction and inelastic impacts between the particles and between them and the walls, energy is dissipated, providing the damping effect. Damping performance is dependent on vibration frequencies and amplitudes, but typically effective over a wide range. [13–15] provide extensive discussion of the basic principles, modelling and influencing parameters of particle damping. Practical applications are reported on in [16, 17], achieving a dramatic reduction of vibration amplitudes.

As a first step towards the integration of particle dampers in displacement pumps, an experimental study was performed with bolt-on damper casings on a 92cc axial piston pump [18]. The casings design was based on an extensive experimental and simulative study of the pump's vibration behaviour, as well as guidelines on particle damper design and performance influencing parameters which were drawn from literature. Figure 2 shows the experimental setup and main sound mitigation result, characterized by the difference in the A-rated sound power level L_{WA}.

The main conclusions drawn from the study were as following:

- A moderate, but systematic sound power level reduction of 0.7 dB(A) on average was achieved for the optimal configuration of casings and particles.
- Steel balls of 2 mm in diameter consistently yielded the best results among the studied particle types.
- Sound power reduction resulted from a combination of damping and decoupling effects, as evidenced by the fact that already empty casings led to a reduction in certain frequency bands, which was increased significantly after filling in particles.
- Insufficiently stiff damper casings resulted in resonant vibrations of the dampers and drastically increased sound emission. The first generation printed plastic casings were replaced with metal ones, which resolved the issue.

For further study of particle damper performance, two approaches were followed, which will be reported on in the following. On the one hand, the concept of mount-on dampers was enhanced with the design of a shell enclosing most of the pump and featuring damper cavities. On the other hand, integrated damper cavities were manufactured in a pump end casing and swash plate.

2 Particle damped shell

2.1 Design

Observing the lessons learned from the bolt-on casings study, the shell was conceptualised to enclose as much of the pump's sound emitting surface as possible. Openings were left for the port connectors, the mounting flange, the control valve and the swivel angle sensor. The inner wall of the shell was placed at a distance of 15 mm from the pump surface, thus determining the thickness of the damping particle layer. While a higher value would be desirable, this was decided for as a compromise between damping effect and space constraints. The cavity

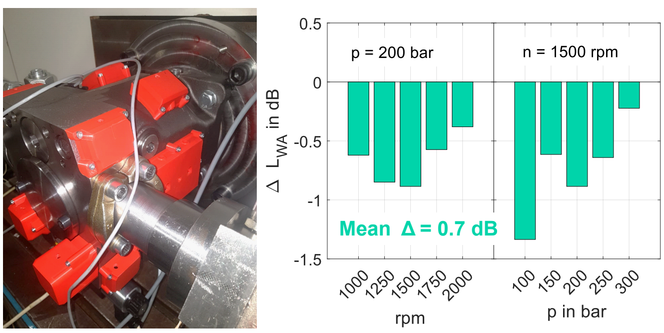

Figure 2: Bolt-on damper casings and achieved sound power level reduction [18]

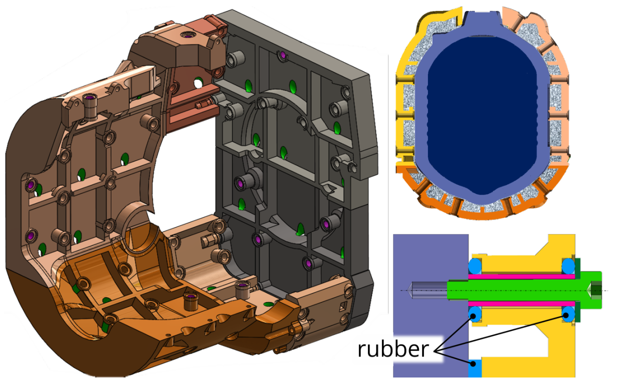

Figure 3: Design of enclosing shell and concept for elastic mounting

under the shell was subdivided into compartments with principal dimensions of approximately 40 mm following the conclusions drawn from [19], observed already in [18]. The subdivision is especially important in the vertical direction, so as to avoid the effect of particle movement being inhibited by the gravity of the particles above. Finally, due to manufacturing constraints the shell was divided into 8 separate parts to be bolted together. The resulting design is shown in Figure 3, with some parts omitted so as to show the inner wall structure.

Particular attention was paid to avoiding resonant vibrations of the shell, which had proved highly problematic in [18]. The solution there had been to employ metal made casings instead of printed plastic, raising their first natural frequencies above 5 kHz, so resonant vibrations of the casings where outweighed with relation to sound power by the particle damping and decoupling effects. Due to the complex and larger scale geometry, this solution was not possible for the shell in this study, with only a 3D printer for plastic material available for the task. To compensate as best as possible by stiffening the structure, a high wall thickness of 10 mm was set, and a carbon fibre reinforced ABS material was chosen for maximum elastic modulus. The compartment walls also serve a secondary function as a reinforcing rib structure. Despite these efforts, a cursory finite element modal analysis using estimated material parameters and boundary conditions found natural frequencies of bending modes starting below 230 Hz, far below a value where resonant vibration could be expected to contribute negligibly to sound power. Problematically low natural frequencies of the thin, multi-part shell structure had to be accepted.

As a further approach to mitigate this problem, the interfaces between pump and shell were devised to be highly elastic, aiming for a decoupling effect in the transmission of pump vibrations towards the shell. As shown in Figure 3, the bolt interfaces were designed such that forces are transmitted through rubber (NBR) O-rings, while still allowing for fastening of the bolts through a steel sleeve (pink). Furthermore, NBR foam tape was also applied to the compartment wall interfaces, on the one hand to provide an elastic mounting, and furthermore to seal the compartments, in order to avoid particle spill.

2.2 Experimental setup and procedure

The pump was installed on a hydraulic test rig in an anechoic chamber, shown in Figure 4. Two types of tests were performed:

On the one hand, sound power measurements at stationary operating points according to the provisions set out in ISO 3744 / DIN 45635-1/26, using 6 microphones on a cuboid enclosing surface limited by 2 reflecting planes. A low reflection line terminator (LRLT) at the end of the high pressure line was included in order to avoid reflections of pressure pulsations from the downstream hydraulic circuit. Apart from airborne sound, structure borne noise signals were measured by means of a laser vibrometer for surface velocity and by piezoelectric accelerometers, as listed in Table 2, and illustrated in Figure 5. Pressure pulsations in the suction and high pressure line were also measured, as well as mechanical and thermal con-

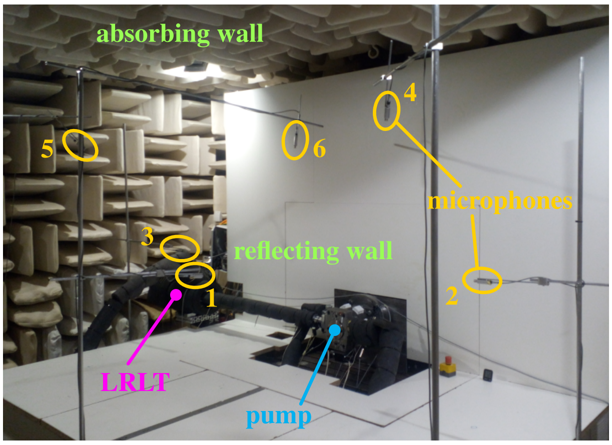

Figure 4: Sound power test rig and structure borne noise signals measured on the pump and damper shell

Table 1: Operating points for sound power measurements

	rev. per minute	high pressure / bar
base set	1000, 1250, ... 2000	200
expanded set	500, 750, ... 2000 500, 1500, 2000	200 50, 100... 300

Table 2: Measured and derived quantities

Symbol	Denotation	Unit
L_{WA}	Sound power level, A-rated	-
v_{EC}	Surface normal velocity on end casing	m/s
$a_{EC,i}$	Triaxial acceleration on end casing surface below shell	m/s^2
a_{PCi}	Normal acceleration on pump casing side wall below shell	m/s^2
a_{PCo}	Normal acceleration on shell surface over pump casing side wall	m/s^2
$H_k(i\Omega)$	Frequency response at point k	m/s/N

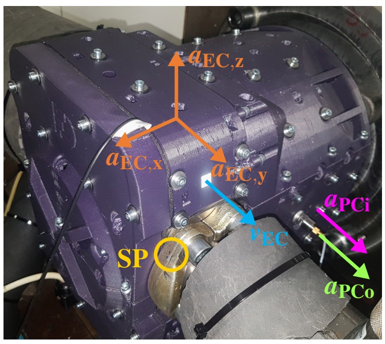

Figure 5: Structure borne noise signals measured on the pump and damper shell

trol and status observation signals from the test rig. Two sets of operating points were run through; a base set for assessment during parameter variation, and an expanded one for in-depth assessment of the most interesting configurations. The operating points are laid out in Table 1. All measurements were carried out at maximum swivel angle and a temperature of $(40 \pm 2)\,°\mathrm{C}$, with two runs for each operating point.

Furthermore, frequency responses were determined on the still pump and shell configurations. Measurement points were defined on spots deemed highly relevant for structure vibrations, based on the operational vibration measurement reported in [18]. At these points k, using the laser vibrometer, the normal surface velocity response $v_k(t)$ to impulse hammer strikes (to the strike point SP on the suction line connection in Figure 5) was measured. The frequency response is the quotient of its Fourier transform and that of the measured impact force $f(t)$,

$$H_k(i\Omega) = \frac{V_k(i\Omega)}{F(i\Omega)}$$

The frequency response is useful for assessing changes in the transmission behaviour, here in particular damping and decoupling, between configurations. The main drawback is that the method only captures frequency dependencies, while it is known that particle dampers can exhibit significant dependency on vibration amplitudes as well.

2.3 Performance

Sound power reduction

After a reference measurement of the regular pump, the shell was mounted. Sound power measurements were performed with the shell empty and with the cavities filled to an increasing degree with 2 mm steel balls, which had shown the best results in [18]. The result is shown in Figure 6. In this diagram, the dots refer to individual measurements, while the bars mark the average for each operating point and configuration. As is evident, the addition of the empty shell increases the emitted sound power greatly for all operating conditions, repeating the result for the plastic damper casings in [18]. The cause can be attributed to resonant vibrations of shell parts as well as the increase in overall sound emitting surface. The former means that the intended decoupling effect was not achieved. Either the rubber coupling elements in Figure 3 are still too stiff, or manufacturing imprecisions and gravity caused direct contact between the shell and the pump casing or the screw sleeves, resulting in a mechanical short circuit. Adding particles mostly compensates for this effect, resulting in a sound power level of approximately the reference value. While it can be stated that the particles result in a clear damping effect, the result in comparison to the reference is unsatisfactory.

As a remedy to the apparently overly stiff attachment of the shell to the pump, the shell was mounted without bolt connections to the pump. Instead, the pump parts connect by bolts to each other, but to the pump only through the NBR foam tape on the cavity and outer wall interfaces of the shell, see Figure 3. Again, sound power measurements were carried out for the empty shell and steel ball filling, with the result on sound power levels depicted in Figure 7.

While the empty shell still leads to a substantial sound power level increase at several operating points, in particular at lower speeds, the effect is much less drastic for this configuration. Meanwhile, a clear damping effect is again observable with particles filled into the cavities, resulting in significant sound power level reductions. Remarkably, the degree of filling has little influence on the mitigation effect, and the results at 50% filling are no worse on average than at 80 or 90%, and not even much worse at 25%. This appears particularly relevant as a full filling of the shell adds a non-trivial 11.5 kg in particle mass.

For a clearer picture of how this result is obtained, the third octave band spectral distribution of sound power level is shown in Figure 8. The multiple lines of same colour again refer to individual measurements and are shown to give a sense of the replicability of the results shown. The comparison between the reference configuration and the empty shell clearly shows a decoupling effect in the higher frequency bands, starting from the one around 2 kHz. Sound power is markedly reduced in all bands above. At the same time, the empty shell produces a significant increase of sound power in several lower frequency bands up to the one at 2 kHz. This is plausibly attributed to resonant vibration at natural frequencies in this range, which are not fully decoupled.

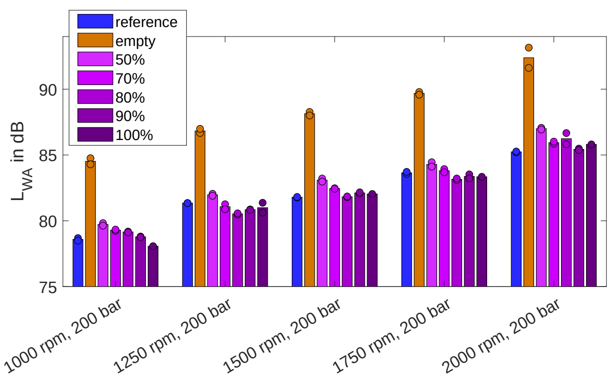

Figure 6: Sound power level for mounted shell filled with steel balls

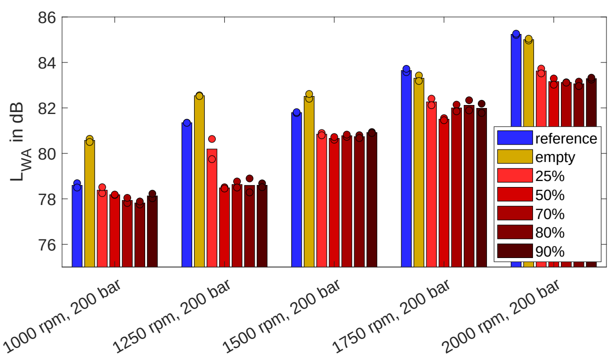

Figure 7: Sound power level for loosely attached shell filled with steel balls

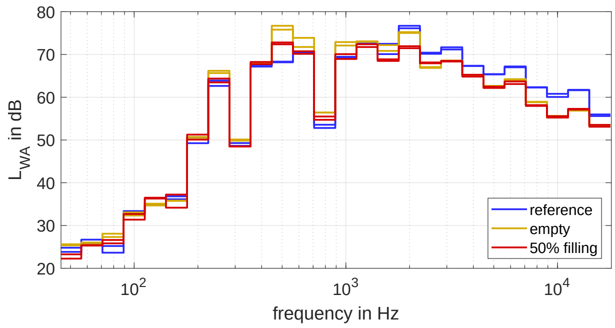

Figure 8: Third octave band spectrum of sound power level for loosely attached shell filled with steel balls at the operating point 1500 rpm, 200 bar

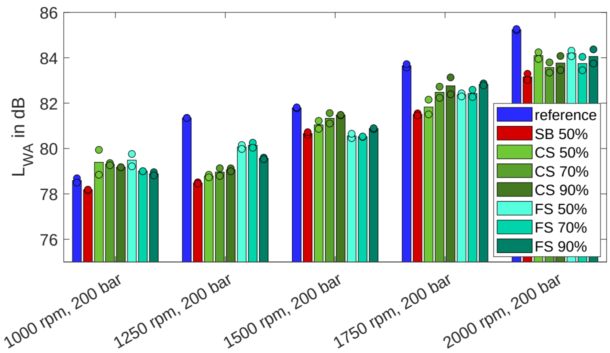

Figure 9: Sound power level for steel balls and sand particles as damping agent; SB.. steel balls; CS.. coarse sand; FS.. fine sand

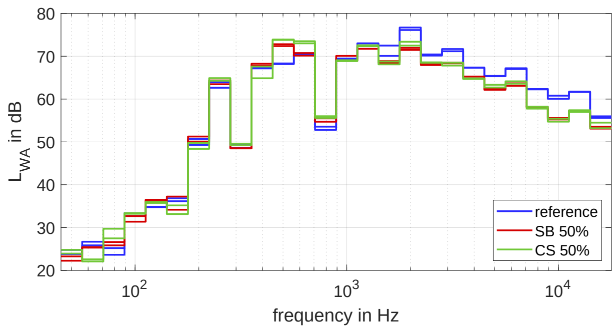

Figure 10: Third octave band spectrum of sound power level at the operating point 1500 rpm, 200 bar, comparing steel balls and coarse sand performance

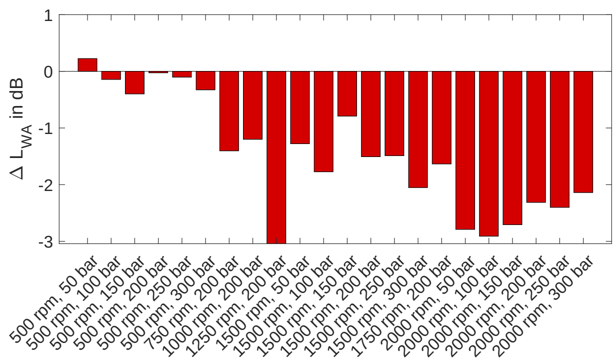

Figure 11: Difference of reference sound power level and the favoured damping configuration of 50% steel ball filling across all examined opterating points

The 50% steel balls filling mitigates these additional sound power contributions significantly, and eliminates it nearly completely in most bands. It also has a strong damping effect on the 2 kHz band, which is the most critical in the reference configuration. The result is the observed overall significantly reduced sound power. At the same time, the sound power spectrum is shifted towards lower frequencies. While the effect is shown for just one operating point here, it repeats qualitatively for all others.

All further studies were done with the loose shell attachment.

While in [18], the steel balls had proven to have the best damping effect compared to cast iron blasting agent of sizes 0.3...2 mm, as well as to irregularly shaped tin drops of 2-4 mm size, the study of the shell performance included an assessment of sand as a damping particle as a possible cost-effective alternative. Two variants were tested: a coarse gravel-sand with 1-2 mm grain size, and fine sand of 0.2-0.6 mm. Figure 9 shows the effects on sound power level. The sound power mitigation effect is reduced for all sand configurations in comparison to the steel balls at most operating points. However, there is still an appreciable and systematic reduction of sound power level with respect to the reference configuration, with the exception of the operating point at 1000 rpm. The exemplary spectrum in Figure 10 shows that the difference between steel and sand particles is mostly the latter having a lesser effect on the additional sound power caused by the shell in the lower frequency bands. This behaviour is found for fine sand as well across operating points.

Finally, Figure 11 presents the obtained sound power level reductions with the preferred damping variant. Across operating points, the average reduction is of -1.5 dB, with a clear tendency for greater reductions at higher revolution speeds. For the operating points at 2000 rpm the reduction is of -2.5 dB.

Sound perception

The above analysis demonstrated how the particle damper shell affects the spectral distribution of the pump's sound emissions. Is it widely known that individual sound perception, i.e. the assessment of sound quality and comfort of sounds, is related in various ways to their spectral distribution [1], while at the same time it is not always a clear function of L_{WA}.

Therefore, an effort was made to assess differences in sound perception of the reference and damped configuration, which may go beyond a comparison of sound power levels. While the research project did not allow for a fully fledged psychoacoustic assessment, which would require extensive randomized sound perception assessments with test subjects, comparative compilations of sounds were shared among colleagues and project partners. There was unanimous agreement that in all cases, the sound from the damped shell configuration is appreciably more comfortable to listen to. Remarkably, even the noise at 500 rpm / 200 bar is generally considered more comfortable for the damper shell configuration, despite the sound power level not being appreciably reduced as per Figure 11.

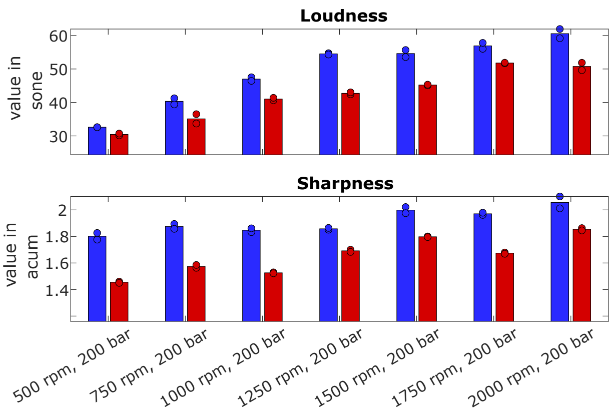

Figure 12: Psychoacoustic functions evaluation for microphone 1 signals

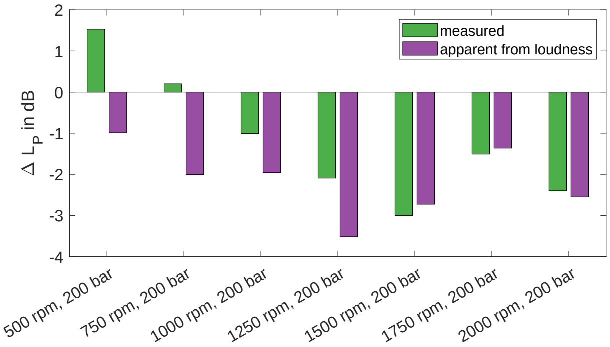

Figure 13: Measured and apparent sound pressure level differences at microphone 1

Sounds are made available to the reader on `https://tud.link/zv4ums`. Each sound file consists of an 8 s record of the reference configuration operation noise, followed by 8 s of that with the 50% steel ball filled shell. For each operating point there is a recording available for both microphone 1 - facing the pump end casing front - and microphone 2 - facing the pump laterally from its left (from positive y in Figure 4). The authors hope for a pleasant hearing experience. It has proved valuable to use as high quality headphones or speakers as available.

For a tentative quantitative assessment of sound perception, the psychoacoustic loudness and sharpness functions were computed[1] for the signals from microphone 1. The result is shown in Figure 12 .

Both values are indeed reduced for all operating points.

The loudness N is a measure intended to capture the average subjectively perceived noise volume more precisely than (A-rated) sound power or pressure levels [1] do. For a sine tone at 1 kHz, the relation to the sound pressure level L_p is [2]

$$N = 2^{\frac{L_p - 40\text{dB}}{10\text{dB}}}$$

With this formula, the loudness differences in Figure 12 are converted to apparent sound pressure level differences

$$\Delta L_p = \frac{10\text{dB}}{\ln 2} \ln \frac{N_{\text{SB50\%}}}{N_{\text{reference}}}$$

In Figure 13 these hypothetical level differences are compared to those computed directly from the measured signals. The difference is significant at lower pump speeds, where meagre or even negative measured level reductions contrast with more pronounced apparent reduction values when derived from loudness. Meanwhile, at higher speeds starting from 1500 rpm the difference between the values is negligible.

The sharpness value quantifies the high frequency contents of a sound, as high frequency noise is generally perceived as particularly unpleasant. There is a clear reduction in sharpness for all operating points, which corresponds to the observations on the sound power spectra in Figure 8.

Similarly to the results in Figure 13, the reduction is most pronounced at the 500 rpm operating point. Both may help explain the above observation of improved sound quality despite the unchanged sound power level for this speed.

Structure borne noise

The acceleration and surface velocity signals are evaluated for a deeper insight into the mechanisms of sound mitigation by the shell. Figure 14 shows the spectra of the 2 signals which were measured on the pump surface for the reference configuration and then on equivalent spots on the shell. Again, 2 spectra are shown for each configuration, representing individual measurements. The capital letters denote the Fourier transforms of the signals listed in Table 2. The frequency resolution was set to $\Delta f = 10\,\text{Hz}$ for readability. The spectra exhibit the characteristic peaks at the pump order frequencies of $f_i = i \cdot rpm \cdot N_{\text{pistons}}$, with $N_{\text{pistons}} = 9$.

The comparison between the reference case and the empty shell corroborates the conclusions from the sound power tertiary band spectra: The empty shell leads to significantly increased vibration amplitudes in the frequency range <1 kHz, $A_{\text{PC,o}}$, and <2 kHz for V_{EC}. This effect is mostly reversed after particles are added. At higher frequencies, already the empty

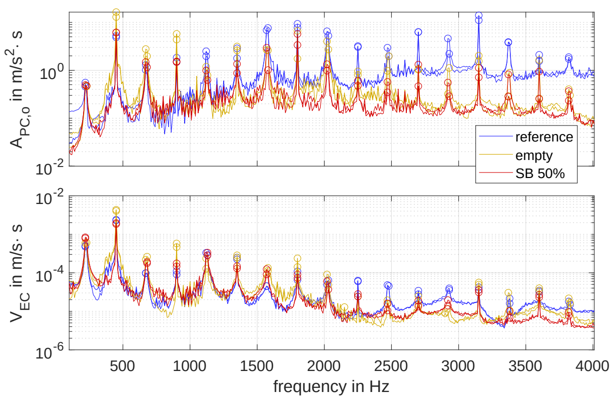

Figure 14: Vibration spectra on the sound emitting surface for 1500 rpm, 200 bar

[1] Computations according to ISO 532-1 / DIN 45631 (Zwicker method) for loudness and DIN 45692 for sharpness

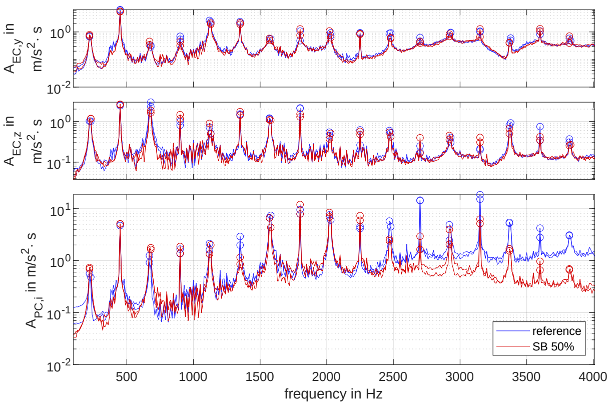

Figure 15: Vibration spectra on the pump surface for 1500 rpm, 200 bar

shell leads to a general reduction of the broadband spectrum and the peaks, starting from 1 kHz on the pump casing, and 2.2 kHz on the end casing. The particles provide a further amplitude reduction at most high frequency peaks of $A_{\mathrm{PC,o}}$. This is true most clearly for the 9th order peak at 2.025 kHz, corresponding to the significant sound power reduction in that band in Figure 8.

The sound power reduction and spectral shift results also pose the question if they are purely due to decoupling effects from the elastically mounted shell and damping of its resonant modes, or if the pump vibration itself is damped. This is assessed in Figure 15, showing the spectra of those acceleration signals which were measured on the pump surface under the shell. The two represented components of A_{EC} on the end casing do indeed appear to be mostly indifferent to the particles. Some minor amplitude reduction is observed at several isolated peaks.

Meanwhile, $A_{\mathrm{PC,i}}$ on the pump casing side wall shows significant and consistent amplitude reduction starting from the 11th order at 2.475 kHz, as well as at the 6th order(1.35 kHz) with the particle damped shell installed.

Frequency response

Measured frequency response functions on measurement points on the pump side walls are presented in Figure 16. The

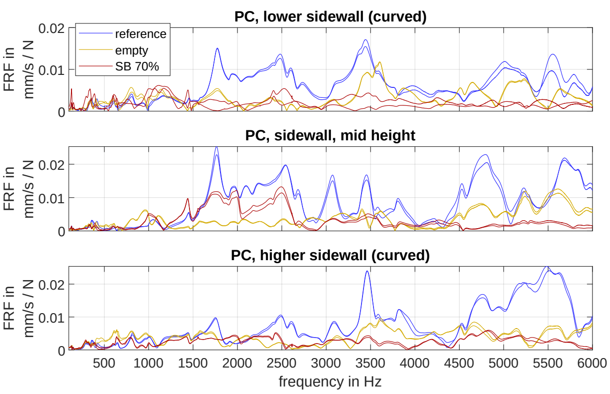

Figure 16: Frequency response measured on pump casing

decoupling effect is well visible with the empty shell leading to near erasure of the original resonant peaks above 1.5 kHz. However, the results with particles are difficult to interpret, and do not correspond well with the observations from the operational measurements.

3 Modified end casing and swash plate

Parallel to the running tests with the shell, a modified swash plate and end casing were manufactured to include cavities for particle damping. The main design motivation here was to exploit available space for cavity placement, which these parts offered so as to allow for a considerable cavity-to-volume fraction. The design concept and implementation on the test rig are depicted in Figure 17.

Cavity covers were made from 5 mm thick steel material, in order to increase stiffness and avoid sound emissions from plate vibrations as much as possible. For test rig experiments, the swash plate had to be installed with a particle filling which could not be feasibly varied, while that was possible for the end casing cavities. Sound power measurements were carried out analogous to Section 2.2. Figure 18 shows the results for various degrees of filling of the end casing cavities.

The pump with the modified, particle damped swash plate and empty end casing cavities has a slightly increased sound power emission compared to the reference configuration. The addition of particles leaves sound power largely unaffected. This

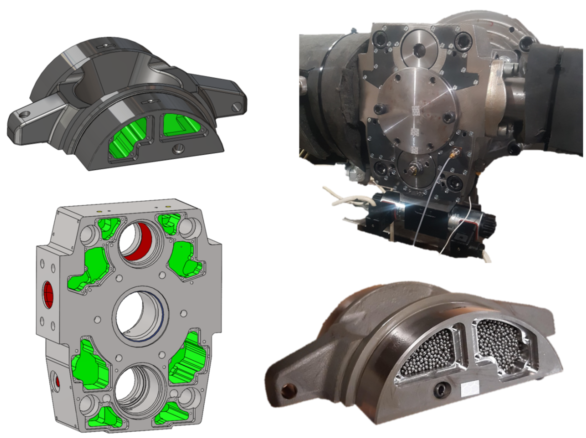

Figure 17: Swash plate and end casing with integrated particle dampers

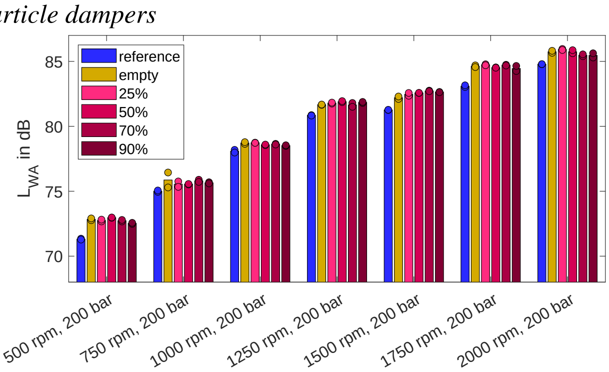

Figure 18: Sound power with integrated particle dampers

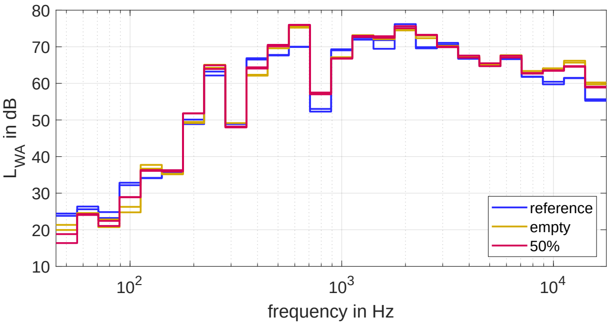

Figure 19: Sound power spectrum with integrated particle dampers at 1500 rpm, 200 bar

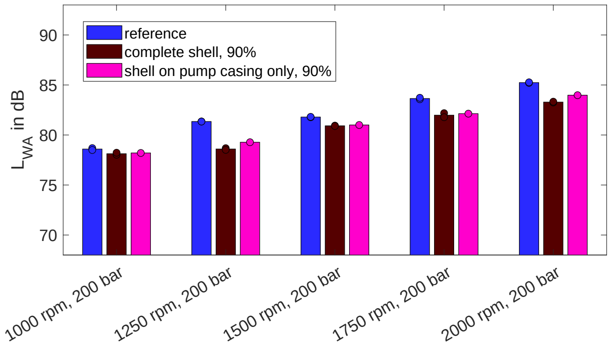

Figure 20: Sound power level comparing the damping shell enclosing the whole pump or the pump casing only

is also true for its spectral distribution, as is demonstrated in Figure 19. Differing from the experiences with the shell as well as with bolt-on casings made of plastic and metal in [18], in this case the particles do not compensate for the additional noise emissions of the empty configuration as compared to the reference.

4 Conclusion and outlook

Two approaches for noise mitigation of displacement pumps through particle damping were implemented and tested.

The elastically mounted and particle damped enclosing shell made of reinforced plastic was able to achieve considerable reductions of sound power depending on the operating point, with a mean value of -1.5 dB and the biggest improvements at high revolution speeds of 2000 rpm with a mean -2.5 dB. This was achieved through a combined mechanism of vibration decoupling between the pump and shell and particle damping. The application of the shell also shifts the spectral distribution of sound power towards lower frequencies, and an improvement of individually perceived sound quality was generally observed among test subjects, although statistically significant listening tests were not performed. The improved sound quality even holds for operating points where the sound power level was unchanged. The application of psychoacoustic valuation functions to the recorded sound signals supports this assessment. The evaluation of structural vibration signals improves the understanding of the mechanisms at work, and demonstrates the decoupling effect, as well as particle damping of the shell and also the pump structure itself. The latter applies to the pump casing at higher frequencies starting around 2.5 kHz, while the vibration of the end casing under the shell was not affected appreciably. Frequency response analysis corroborates the findings on the decoupling mechanism, but proved to be of limited use for assessing the particle damping effect, since it cannot capture its amplitude dependency, and likely the excitation magnitude is too small to yield appreciable damping.

The attempt for a simple improvement of an existing design by introducing damper cavities in available material volume on the other hand proved unsuccessful. Considering the subsequently obtained results from the damper shell regarding spectral distribution of air and structure borne noise, it appears that the sound mitigation effect stems near completely from the dampers on the pump casing. In fact, a measurement series with an incomplete shell leaving the end casing uncovered and enclosing only the pump casing is documented in Figure 20, showing only a minimal difference in emitted sound power between the two configurations. It appears therefore plausible that integrated dampers in the pump housing - which would however require more extensive design modifications - could perform better, although the results with modified pump parts presented here underscore the need for careful preliminary analysis.

For a possible future technical application of the shell, on the one hand room for optimization remains with regards to particle size, cavity design and elastic mounting. The shell as presented here was designed for handy laboratory use, and a technical solution will likely involve fewer parts. At the same time, additive manufacturing might not be feasible and a suitable production method for the required numbers will need to be found and the design adapted accordingly.

Acknowledgement

The presented research activities were carried out in the course of the project "Geräuschminderung in Verdrängereinheiten", funded by Forschungskuratorium Maschinenbau e.V. (FKM-No. 7052400). The authors would like to thank FKM and the Fluid Power Research Fund at VDMA for funding and support.

References

[1] Eberhard Zwicker and Hugo Fastl. *Psychoacoustics: facts and models (2nd, upd. ed.)*. Springer, 1999.

[2] Ville Pulkki and Matti Karjalainen. *Communication Acoustics*. John Wiley & Sons, Ltd, 1 edition, 2015.

[3] Maria Pettersson, Kenneth Weddfelt, and Jan-Ove Palmberg. Methods of Reducing Flow Ripple from Fluid Power Piston Pumps – A Theoretical Approach. *SAE transactions*, 100:158–167, 1991.

[4] Dirk Becher. *Untersuchungen an einer Axialkolbenpumpe mit Ringsystem zur Minderung von Pulsationen*. PhD thesis, TU Dresden, 2003.

[5] Ganesh Kumar Seeniraj and Monika Ivantysynova. Impact of Valve Plate Design on Noise, Volumetric Efficiency and Control Effort in an Axial Piston Pump. In *Proceedings of ASME IMECE2006*, pages 77–84. American Society of Mechanical Engineers Digital Collection, 2006.

[6] Ganesh Kumar Seeniraj and Monika Ivantysynova. A Multi-Parameter Multi-Objective Approach to Reduce Pump Noise Generation. *International Journal of Fluid Power*, 12(1):7–17, January 2011.

[7] Paul Kenneth Kalbfleisch and Monika Ivantysynova. Computational Valve Plate Design in Axial Piston Pumps/Motors. *International Journal of Fluid Power*, pages 177–202, September 2019.

[8] Ganesh Kumar Seeniraj, Zhao , Minming, and Monika Ivantysynova. Effect of Combining Precompression Grooves, PCFV And DCFV on Pump Noise Generation. *International Journal of Fluid Power*, 12(3):53–63, January 2011.

[9] Takao Nishiumi, Takayoshi Ichiyanagi, and Tetsuya Kuribayashi. Development of a novel helmholtz hydraulic silencer for attenuating the pressure ripple from a fixed displacement pump with variable rotational speed. *Proceedings of the 11th IFK, Aachen*, 2018.

[10] Taeho Kim and Monika Ivantysynova. Active vibration control of swash plate-type axial piston machines with two-weight notch least mean square/filtered-x least mean square (lms/fxlms) filters. *Energies*, 10(5):645, 2017.

[11] George E. Totten and Victor J. De Negri. *Handbook of Hydraulic Fluid Technology*. Taylor & Francis Group, Milton, United Kingdom, 2011.

[12] Hang Ye, Yanrong Wang, Bin Liu, and Xianghua Jiang. Experimental study on the damping eect of multi-unit particle dampers applied to bracket structure. *Applied Sciences, vol. 9 (14), p. 2912*, 2019.

[13] Niklas Meyer. *Design of Particle Dampers for Passive Vibration Attenuation*. PhD thesis, TU Hamburg, 2023.

[14] Tobias Ehlers. *Auslegung partikelgedämpfter Strukturbauteile für die Additive Fertigung*. Dissertation, Gottfried Wilhelm Leibniz Universität Hannover, 2023.

[15] Braj Bhushan Prasad, Fabian Duvigneau, Elmar Woschke, and Daniel Juhre. Application and damping mechanism of particle dampers. *PAMM*, 22(1):e202200116, 2023.

[16] Fabian Duvigneau, Sebastian Koch, Elmar Woschke, and Ulrich Gabbert. An effective vibration reduction concept for automotive applications based on granular-filled cavities. *Journal of Vibration and Control*, 24(1):73–82, 2018.

[17] Florian AM Vogel, Sebastian Berger, Ekrem Özkaya, and Dirk Biermann. Vibration suppression in turning $TiAl_6V_4$ using additively manufactured tool holders with specially structured, particle filled hollow elements. *Procedia Manufacturing*, 40:32–37, 2019.

[18] Michael Lenz, Peter Zuppke, Ahmed Shorbagy, and Jürgen Weber. Design strategy for noise reducing particle dampers on hydraulic pumps. *Maha Fluid Power Conference, Lafayette*, 2024.

[19] Thomas Künneke and Detmar Zimmer. Funktionsintegration additiv gefertigter Dämpfungsstrukturen bei Biegeschwingungen. *Additive Fertigung von Bauteilen und Strukturen*, pages 61–74, 2017.